ACADEMIC PRESS

Biochemical and Biophysical Research Communications 294 (2002) 5–10

BBRC

www.academicpress.com

Synthesis, aggregation, neurotoxicity, and secondary structure of various Aβ1–42 mutants of familial Alzheimer's disease at positions 21–23☆

Kazuma Murakami,[a] Kazuhiro Irie,[a,*] Akira Morimoto,[a] Hajime Ohigashi,[a] Mayumi Shindo,[b] Masaya Nagao,[c] Takahiko Shimizu,[d] and Takuji Shirasawa[d]

[a] *Laboratory of Organic Chemistry in Life Science, Division of Food Science and Biotechnology, Graduate School of Agriculture, Kyoto University, Sakyo-ku, Kyoto 606-8502, Japan*

[b] *Applied Biosystems Japan Ltd., Tokyo 104-0032, Japan*

[c] *Division of Integrated Life Science, Graduate School of Biostudies, Kyoto University, Kyoto 606-8502, Japan*

[d] *Department of Molecular Gerontology, Tokyo Metropolitan Institute of Gerontology, Tokyo 173-0015, Japan*

Received 19 April 2002

Abstract

Cerebral amyloid angiopathy (CAA) due to amyloid β (Aβ) deposition is a key pathological feature of Alzheimer's disease (AD), especially in some form of familial Alzheimer's disease (FAD) including hereditary cerebral hemorrhage with amyloidosis—Dutch type. Aβ mainly consists of 40- and 42-mer peptides (Aβ1–40 and Aβ1–42), which accumulate in senile plaques of AD brains and show neurotoxicity for cultured nerve cells. We synthesized all variant forms of Aβ1–42 associated with reported FAD, such as A21G (Flemish), E22Q (Dutch), E22K (Italian), E22G (Arctic), and D23N (Iowa) along with three potential mutants by one point missense mutation (E22A, E22D, and E22V) in a highly pure form, and examined their ability to aggregate and their neurotoxicity in PC12 cells. The mutants at positions 22 and 23 showed potent aggregative ability and neurotoxicity whereas the potential mutants did not, indicating that Aβ1–42 mutants at positions 22 and 23 play a critical role in FAD of Dutch-, Italian-, Arctic-, and Iowa-types. However, Flemish-type FAD needs alternative explanation except the aggregation and neurotoxicity of the corresponding Aβ1–42 mutant. © 2002 Elsevier Science (USA). All rights reserved.

Keywords: Alzheimer's disease; Amyloid β; Cerebral amyloid angiopathy; Familial Alzheimer's disease; Thioflavin-T; MTT; PC12

Alzheimer's disease (AD) is characterized neuropathologically by the progressive deposition of amyloid in the brain parenchyma and cortical blood vessels [1]. This deposition is composed mainly of amyloid β (Aβ) peptides, 40-, and 42-mer peptides (Aβ1–40 and Aβ1–42) which are proteolytically produced from amyloid precursor protein (APP) [2]. Familial Alzheimer's disease (FAD) is related to missense mutations in the APP gene either outside or inside the Aβ coding region. There is a cluster of mutations at positions 21–23 of the Aβ peptides: Flemish (A21G), Dutch (E22Q), Italian (E22K), Arctic (E22G), and Iowa (D23N) [3–7]. These Aβ mutants may play a pathological role in the cerebral amyloid angiopathy (CAA) since these FAD cases characteristically show clinical manifestation of CAA and since Aβ peptides induce neuronal death in vitro by the formation of amyloid fibrils [8]. Recent investigations using synthetic Aβ1–40 peptides with these FAD mutations partly supported this hypothesis [5,6,9,10]. However, there is no report on the FAD-related Aβ1–42 mutants except for the Dutch-type [9]. The investigation

☆ *Abbreviations*: AD, Alzheimer's disease; Aβ, amyloid β; APP, amyloid precursor protein; CAA, cerebral amyloid angiopathy; CD, circular dichroism; DIPEA, *N*,*N*-diisopropylethylamine; DMF, *N*,*N*-dimethylformamide; FAD, familial Alzheimer's disease; HATU, *N*-[(dimethylamino)-1*H*-1,2,3-triazolo[4,5-*b*]pyridin-1-ylmethylene]-*N*-methylmethanaminium hexafluorophosphate *N*-oxide; MALDI-TOF-MS, matrix-assisted laser desorption/ionization time-of-flight mass spectrometry; MTT, 3-(4,5-dimethylthiazol-2-yl)-2,5-diphenyltetrazolium bromide; TFA, trifluoroacetic acid; Th-T, Thioflavin-T.

* Corresponding author. Fax: +81-75-753-6284.
E-mail address: irie@kais.kyoto-u.ac.jp (K. Irie).

0006-291X/02/$ - see front matter © 2002 Elsevier Science (USA). All rights reserved.
PII: S0006-291X(02)00430-8

	1 10 20 30 42
Aβ1-42 (wild-type):	DAEFRHDSGY EVHHQKLVFF AEDVGSNKGA IIGLMVGGVVIA
21G-Aβ1-42 (Flemish):	DAEFRHDSGY EVHHQKLVFF **G**EDVGSNKGA IIGLMVGGVVIA
22Q-Aβ1-42 (Dutch):	DAEFRHDSGY EVHHQKLVFF A**Q**DVGSNKGA IIGLMVGGVVIA
22K-Aβ1-42 (Italian):	DAEFRHDSGY EVHHQKLVFF A**K**DVGSNKGA IIGLMVGGVVIA
22G-Aβ1-42 (Arctic):	DAEFRHDSGY EVHHQKLVFF A**G**DVGSNKGA IIGLMVGGVVIA
23N-Aβ1-42 (Iowa):	DAEFRHDSGY EVHHQKLVFF AE**N**VGSNKGA IIGLMVGGVVIA
22A-Aβ1-42 (GAA/GCA):	DAEFRHDSGY EVHHQKLVFF A**A**DVGSNKGA IIGLMVGGVVIA
22D-Aβ1-42 (GAA/GAT):	DAEFRHDSGY EVHHQKLVFF A**D**DVGSNKGA IIGLMVGGVVIA
22V-Aβ1-42 (GAA/GTA):	DAEFRHDSGY EVHHQKLVFF A**V**DVGSNKGA IIGLMVGGVVIA
Aβ1-40 (wild-type):	DAEFRHDSGY EVHHQKLVFF AEDVGSNKGA IIGLMVGGVV

Fig. 1. Structures of Aβ1–42 mutants synthesized in this study.

of Aβ1–42 species is pivotal to understand the mechanism of FAD because the aggregative ability and neurotoxicity of Aβ1–42 are considerably greater than that of Aβ1–40 [9].

Synthesis of Aβ1–42 with 14 hydrophobic and/or bulky amino acid residues at the C-terminus is quite difficult because it easily aggregates even under weakly acidic and neutral conditions [11]. However, we recently established a highly efficient method for synthesizing long peptides with a continuous flow-type peptide synthesizer (Pioneer) using *N*-[(dimethylamino)-1*H*-1,2,3-triazolo[4,5-*b*]pyridin-1-ylmethylene]-*N*-methylmethanaminium hexafluorophosphate *N*-oxide (HATU) [12], as an activator for Fmoc chemistry [13–15]. We synthesized five FAD-related Aβ1–42 mutants, 21G-, 22Q-, 22K-, 22G-, and 23N-Aβ1–42, along with three potential Aβ1–42 mutants by one point missense mutation at position 22, 22A-, 22D-, and 22V-Aβ1–42, in a highly pure form (Fig. 1) to investigate the role of the Aβ1–42 mutants at positions 21–23 in FAD. This paper describes the aggregation, neurotoxicity in PC12 cells, and secondary structure of these Aβ1–42 mutants.

Materials and methods

General. The following spectroscopic and analytical instruments were used: peptide synthesizer, Pioneer peptide synthesizer (Applied Biosystems, Foster City, CA); HPLC, Waters 600E multisolvent delivery system with 2487 UV Dual λ Absorbance Detector; Waters 625 LC system with 486 UV Tunable Absorbance Detector and 741 Data Module; matrix-assisted laser desorption/ionization time-of-flight mass spectrometry (MALDI-TOF-MS), Applied Biosystems Voyager-DE PRO (Applied Biosystems); thioflavin-T (Th-T) fluorescence, SPECTRA max GEMINI XS-TR (Molecular Devices, Ashiya, Japan); microplate reader, MPR-A4*i* II (TOSOH, Tokyo, Japan); CD spectropolarimeter, J-805 (JASCO, Tokyo, Japan). MALDI-TOF-MS was measured as reported previously [13,15]. HPLC was carried out on a Develosil packed column ODS-UG-5 (20 mm i.d. × 150 mm and 6.0 mm i.d. × 100 mm) (Nomura Chemicals, Seto, Japan).

HATU, piperidine, Fmoc amino acids, Fmoc-Ala-PEG-PS resin, and *N,N*-diisopropylethylamine (DIPEA) were purchased from Applied Biosystems. *N,N*-Dimethylformamide (DMF), trifluoroacetic acid (TFA), 1,2-ethanedithiol, thioanisole, *m*-cresol, diethyl ether (peroxide free), and CH_2Cl_2 were purchased from Nacalai tesque, Kyoto, Japan. MTT reagents were purchased from Sigma.

Synthesis of FAD-related Aβ1–42 mutants. FAD-related Aβ1–42 mutants (Fig. 1) were synthesized in a stepwise fashion on 0.1 mmol of preloaded Fmoc-Ala-PEG-PS resin by Pioneer using the Fmoc method as reported previously [13–15]. The coupling reaction was carried out using Fmoc amino acid (0.4 mmol), HATU (0.4 mmol), and DIPEA (0.8 mmol) in DMF for 30 min. After each coupling reaction, the N-terminus Fmoc group was deblocked with 20% piperidine in DMF.

After completion of the chain elongation, the peptide-resin (ca. 1.1 g) washed with DMF and CH_2Cl_2 was treated with a cocktail containing 16 ml of TFA, 0.4 ml of *m*-cresol, 1.2 ml of ethanedithiol, and 2.4 ml of thioanisole for final deprotection and cleavage from the resin. After 2 h of shaking at room temperature, the suspension was filtered into a 50 ml corning tube (polypropylene, IWAKI). The filtrate was distributed in eight 15 ml corning tubes, to which five volumes of diethyl ether were added. The mixture was allowed to stand at 4 °C for 10 min and then centrifuged (3000 rpm × 5 min) to precipitate the crude peptide. The precipitate was washed with diethyl ether three times.

The crude peptide was purified by RP-HPLC using the Develosil packed column (20 mm i.d. × 150 mm) with elution at 8.0 ml/min by an 100 min linear gradient of 10–40 or 50% CH_3CN in 0.1% NH_4OH. The peak of each FAD-related Aβ1–42 mutant was collected and concentrated in vacuo below 30 °C to remove CH_3CN. Lyophilization gave a corresponding pure Aβ peptide, the purity of which was confirmed by HPLC (>98%).

HPLC analysis after centrifugation. Each FAD-related Aβ1–42 mutant was dissolved in 0.02% NH_4OH at 250 μM. Seventy microliters of each peptide solution was diluted with 630 μl of 50 mM sodium phosphate (pH 7.4) containing 100 mM NaCl to afford a 25 μM peptide solution, which was incubated at 37 °C for 4, 8, 16, or 24 h. After centrifugation at 15,000 rpm in an 1.5 ml Eppendorf microcentrifuge at 4 °C for 10 min, 25 μl of the supernatant was then analyzed by RP-HPLC on the Develosil packed column (6.0 mm i.d. × 100 mm) with elution at 1.0 ml/min by a 40 min linear gradient of 10–40 or 50% CH_3CN in 0.1% NH_4OH. The area of the absorption at 220 nm was integrated and expressed as a percentage of the control.

Thioflavin-T (Th-T) fluorescene assay. Each FAD-related Aβ1–42 mutant was dissolved in 0.02% NH_4OH at 250 μM. After a 10-fold dilution, the resultant 25 μM peptide solution in 50 mM sodium phosphate (pH 7.4) containing 100 mM NaCl was incubated at 37 °C for 4, 8, 16, or 24 h. Ten microliters of each peptide solution was added to 1 ml of 5 mM Th-T in 50 mM Gly-NaOH (pH 8.5). Fluorescence intensity was measured at 450 nm excitation and 482 nm emission by SPECTRA max GEMINI XS-TR as reported previously [16].

Cell culture. Rat pheochromocytoma PC12 cells were obtained from RCB. They were cultured in Dulbecco's modified Eagle's medium (Sigma) containing 5% (v/v) fetal calf serum (Biosciences PTY, Australia), 10% (v/v) horse serum (Gibco, NY), 100 U/ml of penicillin, and 100 μg/ml of streptomycin (Meizi Seika, Tokyo, Japan). For experimental purposes, near-confluent cultures of the cells were plated at approximately 10^4 cells/100 μl/well fresh culture medium in 96-well tissue culture plates coated with collagen, and incubated at 37 °C under 5% CO_2 overnight before experiments.

MTT assay. The reduction of 3-(4,5-dimethylthiazol-2-yl)-2,5-diphenyltetrazolium bromide (MTT) by mitochondrial reductase

was carried out essentially as reported previously [17]. In an 1.5 ml Eppendorf tube, each FAD-related Aβ1–42 mutant was dissolved in 0.02% NH_4OH at concentrations ranging from 0.12 to 120 μM. Each peptide solution was filter-sterilized (0.22 μm), and 10 μl of the resultant solution and 10 μl of PBS (pH 7.4) were, respectively, added to the above-mentioned cell culture in 96-well tissue culture plates, which was incubated at 37 °C under 5% CO_2 for 48 h. After removal of 30 μl of the medium, 10 μl of 5 mg/ml of MTT in PBS (pH 7.4) was added to the cell culture, which was incubated at 37 °C under 5% CO_2 for 4 h. After evacuation of the culture medium, the cell lysis buffer (100 μl/well; 10% SDS, 0.01 M NH_4Cl) was subsequently added to the cells, and the cell lysate was incubated overnight in the dark at room temperature. The colorimetric determination of MTT was made at 600 nm. The absorbance obtained by addition of vehicle was taken as 100%.

Estimation of the secondary structure of the FAD-related Aβ1–42 mutants. Each FAD-related Aβ1–42 mutant was dissolved in 0.02% NH_4OH at 250 μM. Seventy microliters of each peptide solution was diluted with 630 μl of 50 mM sodium phosphate (pH 7.4) containing 100 mM NaCl to afford the 25 μM peptide solution. Each peptide solution was loaded into a 0.1 mm path length quartz cell and circular dichroism (CD) spectra were recorded at 190–260 nm using a J-805 spectropolarimeter (JASCO). The program JWSSE-480 (JASCO) was used for estimation of the secondary structure of each peptide based on the method of Yang et al. [18] using the reference data of Reed, J. and Reed, T.A. [19].

Results and discussion

Synthesis of FAD-related Aβ1–42 mutants

The FAD-related Aβ1–42 mutants along with the potential Aβ1–42 mutants at position 22 (Fig. 1) were synthesized with the Pioneer peptide synthesizer using HATU as an activator for Fmoc chemistry. Final deprotection and cleavage from the resin, followed by purification by RP-HPLC under alkaline conditions (CH_3CN–0.1% NH_4OH) gave each mutant peptide in a highly pure form. The total yields of these peptides were 2–24%, indicating that the average coupling yield of each condensation step was 95–97%. Molecular weights and purity were confirmed by MALDI-TOF-MS measurements (Table 1). An HPLC chromatogram and MALDI-TOF-MS data of 22G-Aβ1–42 (Arctic) are shown in Fig. 2 as a typical example.

Table 1
Yields and MALDI-TOF-MS data of Aβ1–42 mutants synthesized in this study

Aβ mutants	Yield (%)	Obsd. mass	Calcd. mass (MH^+)
Aβ1–42	3.2	4514.43	4515.20
21G-Aβ1–42	22.7	4501.23	4501.08
22K-Aβ1–42	2.3	4514.42	4514.16
22Q-Aβ1–42	6.3	4514.39	4514.12
22G-Aβ1–42	2.1	4443.35	4443.04
23N-Aβ1–42	1.9	4513.94	4514.12
22A-Aβ1–42	5.0	4456.92	4457.07
22D-Aβ1–42	24.0	4501.55	4501.08
22V-Aβ1–42	6.4	4485.49	4485.12

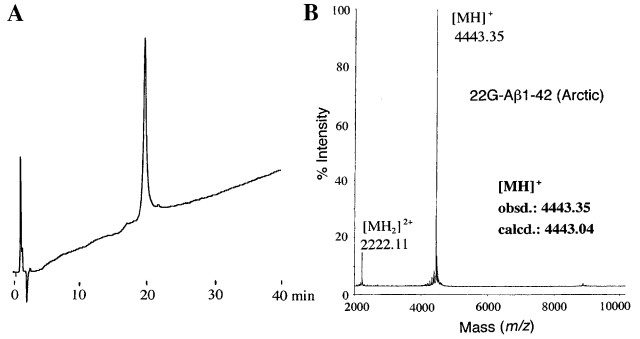

Fig. 2. (A) Chromatogram of 22G-Aβ1–42 (Arctic). The analytical conditions are as follows: Develosil ODS-UG-5 (6.0 mm i.d. × 100 mm), 40-min linear gradient of 10–40% CH_3CN containing 0.1% NH_4OH, 1.0 ml/min, UV 220 nm. (B) MALDI-TOF-MS of 22G-Aβ1–42 (Arctic) by Voyager-DE STR (Applied Biosystems). The peptide dissolved in 0.1% TFA aqueous solution (50 pmol/μl) was mixed with saturated α-cyano-4-hydroxy-cinnamic acid in 50% CH_3CN containing 0.1% TFA at a ratio of 1:1. One microliter of the resultant solution was then measured. Thioredoxin and bovine insulin were used as external references.

Aggregation studies

Aβ aggregations are detectable using Th-T which binds specifically to aggregated forms of Aβ with intense fluorescence. Since the aggregative ability and neurotoxicity of Aβ1–42 are greatest among the Aβ peptides produced from APP, Aβ1–42 is suggested to play a critical role in amyloid formation and the pathogenesis of AD. We could not detect soluble Aβ1–42 after 24 h incubation (Fig. 3A), suggesting that wild-type Aβ1–42 aggregated almost completely after 24 h incubation. Th-T assay gave a similar result (Fig. 3B). On the other hand, Aβ1–40 failed to aggregate even at 24 h after incubation (Fig. 4A and B). These results are consistent with previous findings [9].

Both the centrifugaion and Th-T assay of FAD-related Aβ1–42 mutants showed that 22Q-Aβ1–42 (Dutch) and 22K-Aβ1–42 (Italian) aggregate faster than wild-type Aβ1–42. Although the aggregation of Arctic and Iowa mutants (22G-Aβ1–42 and 23N-Aβ1–42) seemed to be less extensive than that of wild-type Aβ1–42 in the centrifugation assay (Fig. 3A), the rate of aggregation at 4 h after incubation was faster than for wild-type Aβ1–42 by the Th-T assay (Fig. 3B). These results suggest that the FAD-related Aβ1–42 mutants at positions 22 and 23 have more aggregative ability than the wild-type. However, Flemish-type peptide (21G-Aβ1–42) did not aggregate at all like wild-type Aβ1–40, indicating that the Flemish-type needs alternative explanation except the aggregation of the corresponding Aβ1–42 mutant. Wang et al. [20] also reported quite a low level of aggregation of Flemish-type Aβ1–40 mutant peptide. These results and the data on FAD-related Aβ1–40 mutants [5,6,9,10] indicate that the FAD

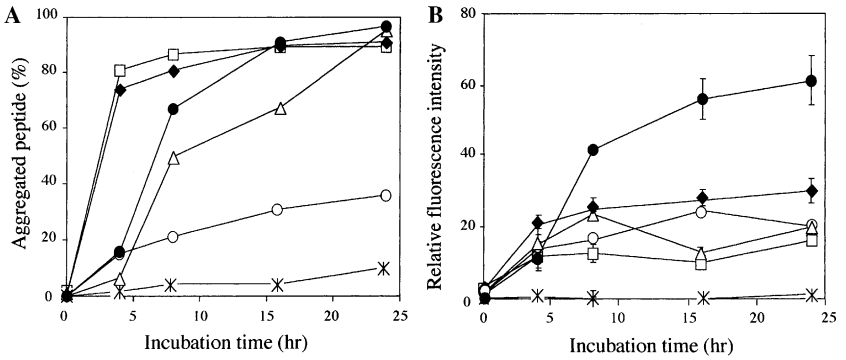

Fig. 3. (A) Aggregation of FAD-related Aβ1–42 mutants estimated by HPLC analysis after centrifugation: (●) wild-type Aβ1–42; (∗) 21G-Aβ1–42 (Flemish); (◯) 22G-Aβ1–42 (Arctic); (◆) 22Q-Aβ1–42 (Dutch); (□) 22K-Aβ1–42 (Italian); (△) 23N-Aβ1–42 (Iowa). (B) Aggregation of FAD-related Aβ1–42 mutants estimated by Th-T fluorescence method [16]: (●) wild-type Aβ1–42; (∗) 21G-Aβ1–42 (Flemish); (◯) 22G-Aβ1–42 (Arctic); (◆) 22Q-Aβ1–42 (Dutch); (□) 22K-Aβ1–42 (Italian); (△) 23N-Aβ1–42 (Iowa).

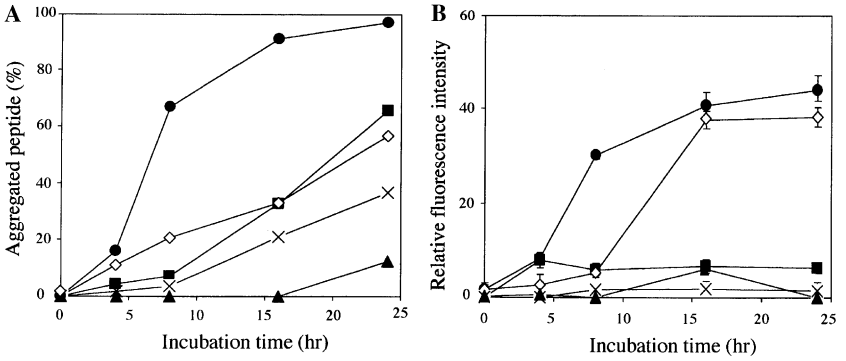

Fig. 4. (A) Aggregation of the potential Aβ1–42 mutants at position 22 estimated by HPLC analysis after centrifugation: (●) wild-type Aβ1–42; (▲) wild-type Aβ1–40; (■) 22A-Aβ1–42; (◇) 22D-Aβ1–42; (×) 22V-Aβ1–42. (B) Aggregation of the potential Aβ1–42 mutants at position 22 estimated by Th-T fluorescence method [16]: (●) wild-type Aβ1–42; (▲) wild-type Aβ1–40; (■) 22A-Aβ1–42; (◇) 22D-Aβ1–42; (×) 22V-Aβ1–42.

mutation at positions 22 and 23 of Aβ peptides increases their aggregative ability.

The aggregative ability of the three potential Aβ1–42 mutants at position 22 (22A-, 22D-, and 22V-Aβ1–42) was considerably less than that of wild-type Aβ1–42 (Fig. 4A and B), suggesting that these mutations would not be responsible for the pathogenesis of the phenotypically related FAD. It is noteworthy that valine at position 22 markedly decreases the ability of Aβ1–42 to aggregate.

Neurotoxicity studies using PC12 cells

The assay of the conversion of MTT to colored formazan by mitochondrial reductase serves as an indirect measurement of cellular proliferation and viability. Rat pheochromocytoma PC12 cells are particularly sensitive to Aβ peptides [17]. After 48 h incubation with each Aβ1–42 mutant, the inhibition of formazan formation was measured at peptide concentrations ranging from 0.01 to 10 μM. The IC_{50} values for the inhibition were determined using the probit procedure [21].

As shown in Table 2, wild-type Aβ1–42 potently inhibited the formation of formazan in PC12 cells at 10^{-6} M, while wild-type Aβ1–40 did not inhibit the formation even at 10^{-5} M. The neurotoxicity data correlate well with the ability of these peptides to aggregate (Fig. 4A and B). The FAD-related Aβ1–42 mutants at position 22 (Dutch, Italian, and Arctic) showed about 10-fold the neurotoxicity of wild-type

Table 2
Neurotoxicity in PC12 cells of FAD-related Aβ1–42 mutants estimated by the MTT assay

FAD-related Aβ mutants	IC_{50}(μM) ± SD
Aβ1–42 (wild-type)	0.97 ± 0.18
21G-Aβ1–42 (Flemish)	1.7 ± 0.26
22Q-Aβ1–42 (Dutch)	0.068 ± 0.011
22K-Aβ1–42 (Italian)	0.14 ± 0.033
22G-Aβ1–42 (Arctic)	0.14 ± 0.045
23N-Aβ1–42 (Iowa)	0.38 ± 0.16
22A-Aβ1–42	2.7 ± 0.13
22D-Aβ1–42	2.9 ± 0.32
22V-Aβ1–42	>100
Aβ1–40 (wild-type)	>100

Aβ1–42, indicating that the Aβ1–42 mutants at position 22 play a critical role in the pathogenesis of these FADs. In contrast, the three potential mutants at position 22 (22A-, 22D-, and 22V-Aβ1–42) were less cytotoxic as the wild-type. Notably, the neurotoxicity of 22V-Aβ1–42 was quite low compared with that of other Aβ1–42 mutants. It can therefore be concluded that these potential mutations would not cause FAD. Melchor et al. [22] recently proposed that a change or loss of charge at position 22 enhances the cytotoxicity of Aβ1–40. However, our results using the Aβ1–42 mutants contradict this hypothesis since the cytotoxicity in PC12 cells of 22V-Aβ1–42 was very weak and that of 22A-Aβ1–42 almost equal to the toxicity of 22D-Aβ1–42. Hydrophobic and/or steric factors at position 22 would affect the aggregation and neurotoxicity of Aβ peptides.

The Iowa-type mutant (23N-Aβ1–42) showed cytotoxicity that was 2–3 fold stronger than the wild-type Aβ1–42, suggesting that the Aβ1–42 mutant at position 23 also plays an important role in the pathogenesis of Iowa-type FAD. However, the cytotoxicity of the Flemish-type Aβ1–42 (21G-Aβ1–42) which hardly aggregated at all as shown in Fig. 3A and B was weaker than that of wild-type Aβ1–42. The cytotoxicity of 21G-Aβ1–42 itself might not be the main cause of Flemish-type FAD.

Secondary structure of Aβ1–42 mutants

Previous structural studies on Aβ peptides suggested that a conformational change from an α-helix or random coil structure to a β-sheet is a key to forming fibrils and inducing cytotoxic effects [23]. The difference in the rate of aggregation among the Aβ mutants examined here would reflect the propensity for adopting the β-sheet structure. To confirm this, the secondary structure of the Aβ mutants was estimated from CD spectra by the method of Yang et al. [18].

As shown in Table 3, CD spectral analyses revealed that the β-sheet content of three FAD-related Aβ1–42 mutants (Dutch, Arctic, and Iowa) is considerably high (ca. 50%). These results are consistent with the aggregative ability and neurotoxicity. The Flemish-type Aβ1–42 mutant whose ability to aggregate and neurotoxicity was quite low contained fewer β-sheets (24%) than wild-type Aβ1–42 (35%). Moreover, all potential Aβ1–42 mutants at position 22 had fewer β-sheets than wild-type Aβ1–42. These results support the hypothesis that the β-sheet structure of Aβ peptides is closely related to their aggregation and neurotoxicity [23].

However, the β-sheet content (32%) of 22K-Aβ1–42 (Italian), whose aggregative ability and neurotoxicity exceeded that of wild-type Aβ1–42, was not so high compared with wild-type Aβ1–42 (35%), instead turn content (56%) increased significantly. This indicates that the β-sheet is not the exclusive secondary structure related to the aggregation and neurotoxicity of Aβ peptides. Since a Lys–Asp sequence is often found in two-residue β-turn [24], the formation of β-turn at positions 22 and 23 followed by intramolecular antiparallel β-sheets might induce the aggregation of Aβ peptides to form fibrils resulting in neurotoxicity.

In conclusion, we synthesized all Aβ1–42 mutants related to FAD along with three potential mutants at position 22 in a highly pure form, and suggested that these Aβ1–42 mutants play a critical role in the pathogenesis of FAD with CAA. Although Miravalle et al. [5] recently proposed that the Aβ1–40 mutant is a more crucial determinant than the corresponding Aβ1–42 mutant in Dutch-type FAD since 22Q-Aβ1–42 did not show any neurotoxic effects, our results using highly pure 22Q-Aβ1–42 contradict theirs. To understand the mechanism of FAD, attention should also be directed at Aβ1–42 mutants as well as Aβ1–40 mutants. However, it might be preferable for mutations at position 21 of Aβ peptides to be differentiated from those at positions 22 and 23 since the Flemish-type Aβ1–42 mutant did not show potent aggregative ability or neurotoxicity.

Table 3
Secondary structure of the FAD-related Aβ1–42 mutants estimated based on CD spectra

Aβ mutants	Secondary structure (%)			
	β-Sheet	Turn	α-Helix	Random
Aβ1–42	35	9	4	52
21G-Aβ1–42	24	26	0	50
22K-Aβ1–42	32	56	2	10
22Q-Aβ1–42	51	43	6	0
22G-Aβ1–42	48	25	0	27
23N-Aβ1–42	52	23	3	22
22A-Aβ1–42	33	36	2	29
22D-Aβ1–42	23	23	2	52
22V-Aβ1–42	22	76	2	0
Aβ1–40	31	2	22	45

Acknowledgments

The research was partly supported by a Grant-in-Aid for Scientific Research (B) (No.13460048) (K.I.) and Special Coordination Funds (H.O.) from the Ministry of Education, Culture, Sports, Science, and Technology, the Japanese Government.

References

[1] D.J. Selkoe, The cell biology of β-amyloid precursor protein and presenilin in Alzheimer's disease, Trends Cell Biol. 8 (1998) 447–453.

[2] T. Iwatsubo, A. Odaka, N. Suzuki, H. Mizusawa, N. Nukina, Y. Ihara, Visualization of a 42(43) and a 40 in senile plaques with end-specific Aβ monoclonals: evidence that an initially deposited species is Aβ 42(43), Neuron 13 (1994) 45–53.

[3] L. Hendriks, C.M. van Duijn, P. Cras, M. Cruts, W. van Hul, F. van Harskamp, A. Warren, M.G. McInnis, S.E. Antonarakis, J.-J. Martin, A. Hofman, C.V. Broeckhoven, Presenile dementia and cerebral haemorrhage linked to a mutation at codon 692 of the β-amyloid precursor protein gene, Nature Genet. 1 (1992) 218–221.
[4] E. Levy, M.D. Carman, I.J. Fernandez-Madrid, M.D. Power, I. Lieberburg, S.G. van Duinen, G.Th.A.M. Bots, W. Luyendijk, B. Frangione, Mutation of the Alzheimer's disease amyloid gene in hereditary cerebral hemorrhage, Dutch type, Science 248 (1990) 1124–1126.
[5] L. Miravalle, T. Tokuda, R. Chiarle, G. Giaccone, O. Bugiani, F. Tagliavini, B. Frangione, J. Ghiso, Substitutions at codon 22 of Alzheimer's Aβ peptide induce diverse conformational changes and apoptotic effects in human cerebral endothelial cells, J. Biol. Chem. 275 (2000) 27110–27116.
[6] C. Nilsberth, A. Westlind-Danielsson, C.B. Eckman, M.M. Condron, K. Axelman, C. Forsell, C. Stenh, J. Luthman, D.B. Teplow, S.G. Younkin, The 'Arctic' APP mutation (E693G) causes Alzheimer's disease by enhanced Aβ protofibril formation, Nature Neurosci. 4 (2001) 887–893.
[7] T.J. Grabowski, H.S. Cho, J.P. Vonsattel, G.W. Rebeck, S.M. Greenberg, Novel amyloid precursor protein mutation in an Iowa family with dementia and severe cerebral amyloid angiopathy, Ann. Neurol. 49 (2001) 697–705.
[8] C.J. Pike, D. Burdick, A.J. Walencewicz, C.G. Glabe, C.W. Cotman, Neurodegeneration induced by β-amyloid peptides in vitro: the role of peptide assembly state, J. Neurosci. 13 (1993) 1676–1687.
[9] J. Davis, W.E. van Nostrand, Enhanced pathologic properties of Dutch-type mutant amyloid β-protein, Proc. Natl. Acad. Sci. USA 93 (1996) 2996–3000.
[10] W.E. van Nostrand, J.P. Melchor, H.S. Cho, S.M. Greenberg, G.W. Rebeck, Pathogenic effects of D23N Iowa mutant amyloid β-protein, J. Biol. Chem. 276 (2001) 32860–32866.
[11] D. Burdick, B. Soreghan, M. Kwon, J. Kosmoski, M. Knauer, A. Henschen, J. Yates, C. Cotman, C. Glabe, Assembly and aggregation properties of synthetic Alzheimer's A4/β amyloid peptide analogs, J. Biol. Chem. 267 (1992) 546–554.
[12] L.A. Carpino, 1-Hydroxy-7-azabenzotriazole. An efficient peptide coupling additive, J. Am. Chem. Soc. 115 (1993) 4397–4398.
[13] K. Irie, K. Oie, A. Nakahara, Y. Yanai, H. Ohigashi, P.A. Wender, H. Fukuda, H. Konishi, U. Kikkawa, Molecular basis for protein kinase C isozyme-selective binding: the synthesis, folding, and phorbol ester binding of the cysteine-rich domains of all protein kinase C isozymes, J. Am. Chem. Soc. 120 (1998) 9159–9167.
[14] H. Fukuda, T. Shimizu, M. Nakajima, H. Mori, T. Shirasawa, Synthesis, aggregation, and neurotoxicity of the Alzheimer's Aβ1–42 amyloid peptide and its isoaspartyl isomers, Bioorg. Med. Chem. Lett. 9 (1999) 953–956.
[15] M. Shindo, K. Irie, A. Nakahara, H. Ohigashi, H. Konishi, U. Kikkawa, H. Fukuda, P.A. Wender, Toward the identification of selective modulators of protein kinase C (PKC) isozymes: establishment of a binding assay for PKC isozymes using synthetic C1 peptide receptors and identification of the critical residues involved in the phorbol ester binding, Bioorg. Med. Chem. 9 (2001) 2073–2081.
[16] H. Naiki, F. Gejyo, Kinetic analysis of amyloid fibril formation, Meth. Enzymol. 309 (1999) 305–318.
[17] M.S. Shearman, C.I. Ragan, L.L. Iversen, Inhibition of PC12 cell redox activity is a specific, early indicator of the mechanism of β-amyloid-mediated cell death, Proc. Natl. Acad. Sci. USA 91 (1994) 1470–1474.
[18] J.T. Yang, C.-S.C. Wu, H.M. Martinez, Calculation of protein conformation from circular dichroism, Meth. Enzymol. 130 (1986) 208–269.
[19] J. Reed, T.A. Reed, A set of constructed type spectra for the practical estimation of peptide secondary structure from circular dichroism, Anal. Biochem. 254 (1997) 36–40.
[20] Z. Wang, R. Natté, J.A. Berliner, S.G. Van Duinen, H.V. Vinters, Toxicity of Dutch (E22Q) and Flemish (A21G) mutant amyloid β proteins to human cerebral microvessel and aortic smooth muscle cells, Stroke 31 (2000) 534–538.
[21] H.G. James, Probit procedure, in: T.H. Jane, A.C. Kathryn (Eds.), SAS User's Guide, SAS Institute, Cary, NC, 1979, pp. 357–360.
[22] J.P. Melchor, L. McVoy, W.E. van Nostrand, Charge alterations of E22 enhance the pathogenic properties of the amyloid β-protein, J. Neurochem. 74 (2000) 2209–2212.
[23] L.C. Serpell, Alzheimer's amyloid fibrils: structure and assembly, Biochim. Biophys. Acta 1502 (2000) 16–30.
[24] B.L. Sibanda, J.M. Thornton, β-Hairpin families in globular proteins, Nature 316 (1985) 170–174.